Applications of Dibaryon/Dimer fields in low energy EFTs

Jaber Balal Habashi

UMass Amherst, ACFI

INT23-1B May 23, 2023

jbhabashi@umass.edu

Outline

1. A Review of Nucl-EFTs
2. NN with Dibaryon
3. Resonances with Dimer
4. Conclusion

My highlights in the history of Nucl-EFTs

- Weinberg (68) [1]: Non-linear realization of chiral symmetry.
- Weinberg (79) [2]: The first EFT for pion interactions. This was the beginning of χPT with Weinberg power counting (WPC).
- Manohar and Georgi (84) [3]: Introduced the naive dimensional analysis (NDA).
- Weinberg (90-91) [4, 5]: The first EFT (χEFT) for pions and nucleons. The key features were infrared enhancement and the introduction of contact interactions.
- KSW (96-98) [6–8]: Inconsistency in WPC (divergence term with a factor of m_π^2). KSW introduced a PC with perturbative pions.
- van Kolck (98) [9]: A general EFT approach to the short range forces. Later, the idea from this paper and KSW papers developed to become what we know today as the Standard Pionless EFT.

What is an EFT?

- In EFTs external (not internal loop) momenta are important!
- Four main building blocks of any EFT:
  - Fields (particles) that appear in a scattering process
  - Symmetries of the scattering process.
  - Typical three momenta, $\vec{p} \sim M_{\text{lo}}$, of the external particles in the scattering process.
  - The breakdown scale of EFT, M_{hi}, is the scale at which a new physics (particle) appears in the process.
- We build the most general Lagrangian $(d \geq 4)$ according to the symmetry considerations and in terms of the given fields.
- In an EFT, power counting (PC) exploits the ratio(s) of scales that appear in scattering. The PC (if consistent) determines orders of operators in a perturbation based on the ratio(s) of scales.

Various PC in Nucl-EFTs

- Scales in the NN system:

$$\Lambda_\chi = 4\pi f_\pi \sim M_{QCD} \sim m_N \sim 1 \text{ GeV}$$

$$\Lambda_{NN} = \frac{16\pi\, f_\pi^2}{g_A^2 m_N} \sim k_0 \sim 300 \text{ MeV}$$

$$f_\pi \sim m_\pi \sim 100 \text{ MeV}$$

$$|\kappa| \approx \frac{1}{|a_s|} \sim \mathcal{O}(10) \text{ MeV}$$

Pionless

KSW

Weinberg

- List of popular PC in Nucl-EFTs (historically LO attempts)
  - WPC [4, 5] or NDA [3] with Non-perturbative pions
  - KSW PC [6–8] with perturbative pions
  - Standard Pionless PC [9]
- $+$ . . . (for a recent review see van Kolck (20) [10])

The WPC and NDA

- The WPC focuses on external momenta, and usage of f_π and $M_{\text{hi}} \sim 1$ GeV are implicit.
- An operator consistent with NDA, with $\Lambda = \Lambda_\chi = 4\pi f_\pi$, is given by [3, 10]

$$\mathcal{O}_{A,B,C,D} = \left(\frac{\pi}{f_\pi}\right)^A \left(\frac{\psi}{f_\pi\sqrt{\Lambda}}\right)^B \left(\frac{g\,G_\mu}{\Lambda}\right)^C \left(\frac{k, m_\pi}{\Lambda}\right)^D f_\pi^2\,\Lambda_\chi^2$$

- NDA also put tree and loop diagrams in different classes sorted by powers of external momenta and fields.
- Factors of 4π counting in loop diagrams are important for understanding how the NDA or equivalently the WPC work.
- For two-body contact interactions $(A, B, C, D) = (0, 4, 0, 2n)$ the coefficients are

$$C_{2n}\,k^{2n} \propto \frac{1}{f_\pi^4\,\Lambda^2}\,\frac{k^{2n}}{\Lambda^{2n}}\,f_\pi^2\,\Lambda_\chi^2 = \frac{k^{2n}}{f_\pi^2\,\Lambda^{2n}} = \frac{4\pi}{\Lambda}\,\frac{k^{2n}}{f_\pi\,\Lambda^{2n}} \sim \frac{4\pi}{m_N}\,\frac{1}{M_{\text{lo}}\,M_{\text{hi}}^{2n}}\,M_{\text{lo}}^{2n}$$

NDA vs KSW vs Standard Pionless PC: Two-body

- NDA (Non-perturbative)
  - PC for contact interactions: $C_{2n}\,k^{2n} \sim \frac{4\pi}{m_N}\frac{1}{M_{\text{lo}}\,M_{\text{hi}}^{2n}}\,M_{\text{lo}}^{2n}$
  - Pions are non-perturabtive.
  - Need consistency and regulator-dependency check.
- KSW and Standard Pionless EFT (Perturbative except for C_0)
  - For S waves: $C_{2n}\,k^{2n} \sim \frac{4\pi}{m_N}\frac{1}{M_{\text{lo}}^{n+1}\,M_{\text{hi}}^{n}}\,M_{\text{lo}}^{2n}$ (Promotion relative to NDA)
  - For S-D channel: $C_{2n}\,k^{2n} \sim \frac{4\pi}{m_N}\frac{1}{M_{\text{lo}}\,M_{\text{hi}}^{2n}}\,M_{\text{lo}}^{2n}$ (No-change relative to NDA)
  - For all higher waves: $C_{2n}\,k^{2n} \sim \frac{4\pi}{m_N}\frac{1}{M_{\text{hi}}^{2n+1}}\,M_{\text{lo}}^{2n}$ (Demotion relative to NDA)
  - In KSW PC pions are perturabtive due to $\frac{m_\pi}{\Lambda_{NN}} \sim \frac{1}{2}$

An Example: the shallow S-wave state

- Bound or Virtual state (for simplicity, I focus only on contact parts)
  - The renormalized contact interaction is: $C_0^R \sim \dfrac{4\,\pi}{m_N}\dfrac{1}{M_{\text{lo}}}$.
  - Finite value of each loop (with the unitary term $i\,k$) scales as $I_0^{[\mathtt{fin}]} \sim \dfrac{m_N}{4\,\pi}M_{\text{lo}}$.
  - Higher-derivative interactions: for example, the renormalized vertex with two derivatives, appears at **NNLO** in NDA $C_2^R \sim \dfrac{4\,\pi}{m_N}\dfrac{1}{M_{\text{lo}}\,M_{\text{hi}}^2}$ and at **NLO** in KSW and Pionless $C_2^R \sim \dfrac{4\,\pi}{m_N}\dfrac{1}{M_{\text{lo}}^2\,M_{\text{hi}}}$.
- Diagrams and T matrix

$-i\,T^{(0)}$:

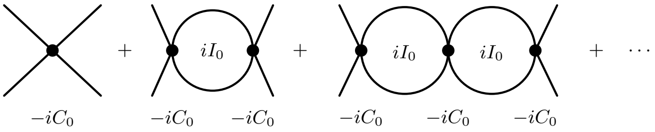

An Example: the shallow S-wave state

- Bound or Virtual state (for simplicity, I focus only on contact parts)
  - The renormalized contact interaction is: $C_0^R \sim \frac{4\pi}{m_N}\frac{1}{M_{\text{lo}}}$.
  - Finite value of each loop (with the unitary term $i\,k$) scales as $I_0^{[\mathtt{fin}]} \sim \frac{m_N}{4\pi} M_{\text{lo}}$.
  - Higher-derivative interactions: for example, the renormalized vertex with two derivatives, appears at **NNLO** in NDA $C_2^R \sim \frac{4\pi}{m_N}\frac{1}{M_{\text{lo}}\,M_{\text{hi}}^2}$ and at **NLO** in KSW and Pionless $C_2^R \sim \frac{4\pi}{m_N}\frac{1}{M_{\text{lo}}^2\,M_{\text{hi}}}$.
- Diagrams and T matrix

$$T^{(0)} = C_0 + C_0\,I_0\,C_0 + C_0\,I_0\,C_0\,I_0\,C_0 + \ldots = \frac{1}{1/C_0 - I_0} = -\frac{4\pi}{m_N}\frac{1}{-1/a_0 - i\,k + \ldots}$$

Problems in early Nucl-EFTs

- Regulator dependent
  - The given LECs are not enough to make amplitudes or phase shifts regulator independent (KSW (96), Nogga et al. (05) [11]).
  - Remedy: these regulator-dependent behaviors can be removed by promoting LECs.
- Convergence issues
  - In WPC, the ${}^1S_0$ channel EFT has a strong deviation from data (Nogga et al. (05)).
  - In KSW PC there are also slow channels (Fleming et al. (99) [12]).
  - Remedy: again promoting LECs may help!
- The PC for many-body systems is not clear yet (Yang et al. (19) [13]).

Outline

Motivation

- For both perturbative and non-perturbative pions, modifications are needed in the lower partial wave channels where the tensor part of OPE is attractive, such as the ${}^3P_0$ channel (Fleming et al. (99), Nogga et al. (05), Kaplan (19) [14]).
- In order to have a better convergence with perturbative pions the physics of energies above pion mass should be included (Kaplan & Steele (99) [15]).
- PC of contact LECs have been changed in order to solve regulator dependency and convergence problems (Nogga et al. (05), Peng et al. (20) [16]).
- Adding dibaryon field can account for most of the physics of energies above the pion mass (Kaplan (96) [17], Sanchez et al. (18) [18]).

Adding Dibaryons to NN scattering

- Symmetries
  - Baryon Number conservation,
  - Lorentz invariant (= Galilean + reparametrization)
  - Parity and time-reversal invariant
  - Chiral symmetry
- Degrees of freedom: N (Nucleon), $\vec{\pi}$ (Pion) and ϕ (Dibaryon).
- The most general Lagrangian

$$\begin{aligned}\mathcal{L} =& \mathcal{L}_0^N + \mathcal{L}_0^\pi + \eta^{(s)} \phi_{i,a}^{(s)\dagger} \left[i\partial_0 + \frac{\vec{\nabla}^2}{4m_N} - \left(\Delta^{(s)} + \omega^{(s)}\, m_\pi^2 \right) \right] \phi_{i,a}^{(s)} \\ & - \frac{g_A}{2f_\pi} N^\dagger \tau_a \left(\vec{\sigma} \cdot \vec{\nabla}\pi_a \right) N - \frac{4\pi}{m_N} \left(C^{(s)} + D^{(s)}\, m_\pi^2 \right) \left(N^T P_{i,a}^{(s)} N \right)^\dagger \left(N^T P_{i,a}^{(s)} N \right) \\ & + \sqrt{\frac{4\pi}{m_N}} \left(g^{(s)} + h^{(s)}\, m_\pi^2 \right) \left(\phi_{i,a}^{(s)\dagger} N^T P_{i,a}^{(s)} N + \mathrm{H.c.} \right) + \ldots ,\end{aligned}$$

S-Waves: Convergence in KSW PC

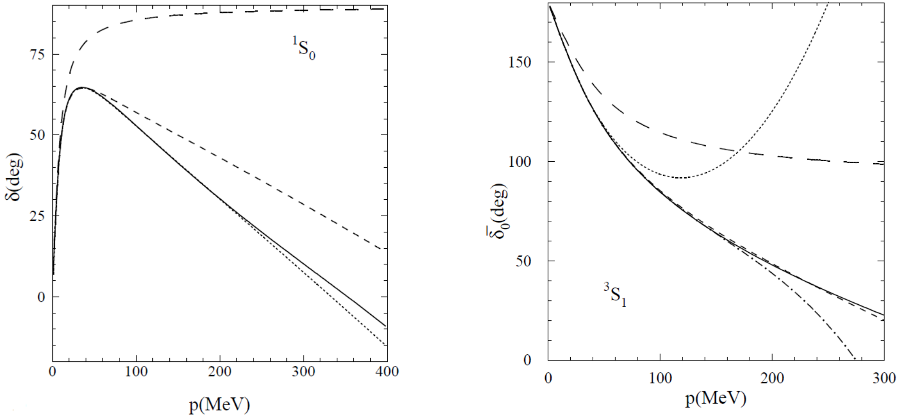

Figure 1: LO (long dashed), NLO (short dashed), and N^{2}LO (dotted) phase shifts for the KSW PC. Figures from Fleming et al. (99).

S-Waves: Convergence in KSW PC

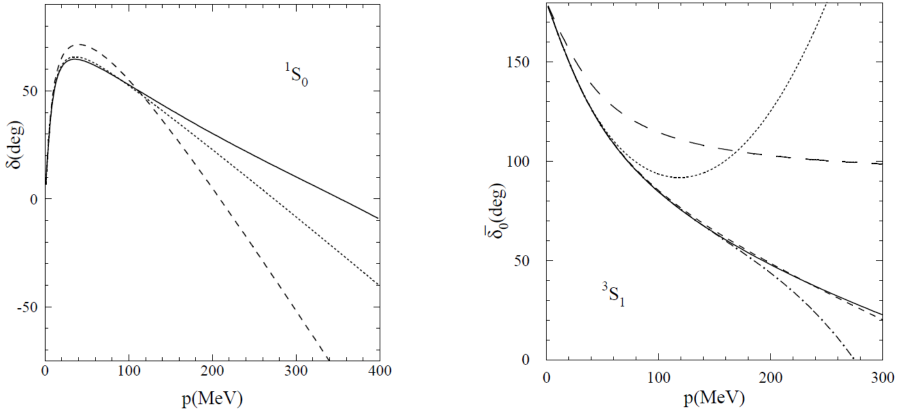

Figure 1: LO (long dashed), NLO (short dashed), and N^{2}LO (dotted) phase shifts for the KSW PC. Figures from Fleming et al. (99).

S-Waves: Including the amplitude zero

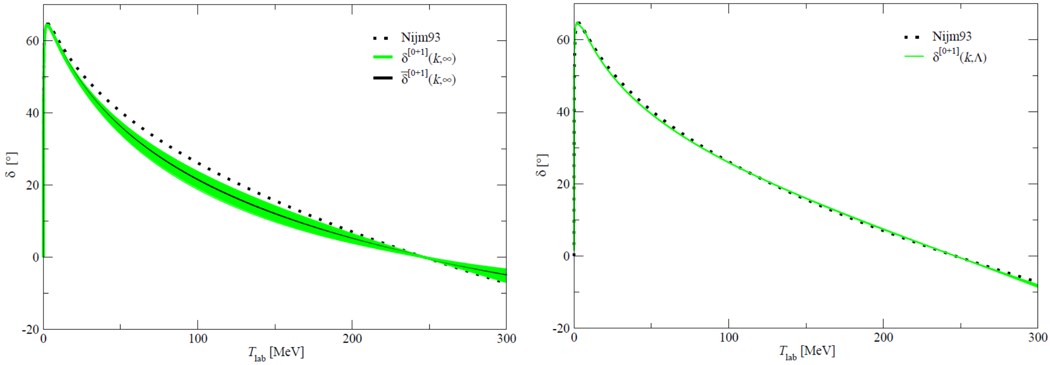

Figure 2: Phase shift (solid line with green band) for the ${}^1S_0$ channel with Pionless (left) and Chiral (right) EFTs. The chiral EFT results were first given by Kaplan (96). Figures from Sanchez et al. (18).

S-Waves: Power Counting

PC	M_{hi}	M_{lo}	LO	NLO
KSW	Λ_{NN}	$m_\pi,\ \lvert\kappa_0\rvert$	C_0	OPE, $C_2,\ D_2$
W'	$M_{\rm QCD}$	$\Lambda_{NN},\ m_\pi$	OPE, $C_0,\ D_2$	C_2
Here	$M_{\rm QCD}$	$\Lambda_{NN},\ k_0,\ (m_\pi^2 M_{\rm QCD})^{1/3}$	$C_0,\ \Delta,\ g_0$	OPE, $C_2,\ D_2,\ \omega,\ h_0$

- Power counting of LO and NLO LECs:

$$g_0^{(0)} \sim \sqrt{\frac{M_{\text{lo}}}{m_N}}\,, \quad C_0^{(0)} \sim \frac{1}{M_{\text{lo}}}\,, \quad \Delta^{(0)} \sim \frac{M_{\text{lo}}^2}{m_N}\,, \quad C_2^{(1)} \sim \frac{1}{M_{\text{lo}}^2 M_{\text{hi}}}$$

$$g_0^{(1)}, h_0^{(1)}\, m_\pi^2 \sim \frac{M_{\text{lo}}}{M_{\text{hi}}}\sqrt{\frac{M_{\text{lo}}}{m_N}}\,, \quad C_0^{(1)}, D_2^{(1)}\, m_\pi^2 \sim \frac{1}{M_{\text{hi}}}\,, \quad \Delta^{(1)}, \omega^{(1)}\, m_\pi^2 \sim \frac{M_{\text{lo}}^3}{m_N M_{\text{hi}}}\,.$$

S-Waves: LO with resummed contact+Dibyaron

- The Renormalized LO T matrix

$$T^{(0)}(k) = -\frac{4\pi}{m_N}\frac{1}{k\cot\delta^{(0)}(k) - ik}$$

$$k\cot\delta^{(0)}(k) = \frac{b_0 + b_2\,k^2}{1 - k^2/k_0^2}$$

- The LO LECs $C_0^{(0)}$, $\Delta^{(0)}$ and $g_0^{(0)}$ are given by b_0, b_2, k_0 and the cutoff Λ.

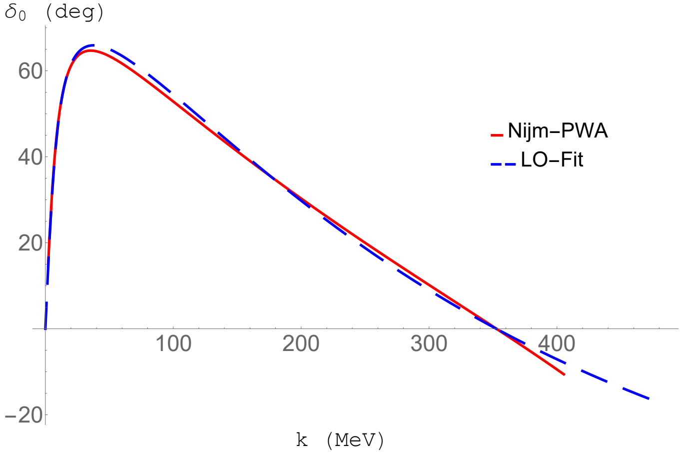

Figure 3: LO EFT phase shift (blue dashed line) for the $^1S_0$ channel.

S-Waves: NLO with perturbative pions

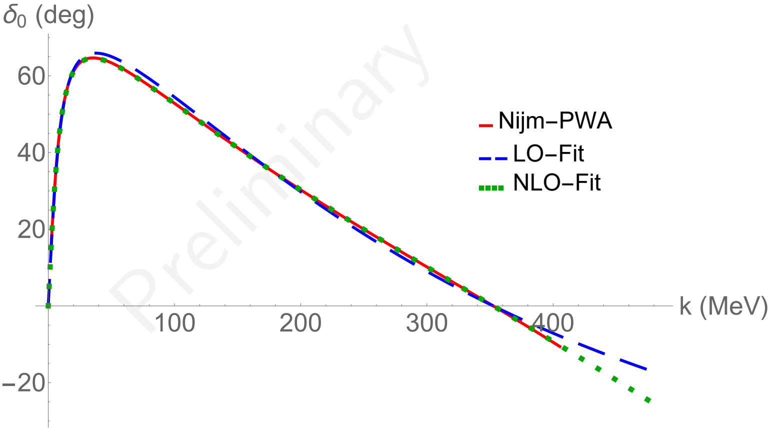

Figure 4: LO (blue dashed) and NLO (green dotted) EFT phase shifts for the $^1S_0$ channel. In collaboration with S. Fleming, M. Sanchez Sanchez, and U. van Kolck.

P-waves: LECs and PC

- PC for LECs with $n, m \geq 1$ (JBH (22) [19])

$$C_{2n} \sim \frac{1}{M_{\text{lo}} M_{\text{hi}}^{2n}}\,, \qquad D_{2n+2m}\, m_\pi^{2m} \sim \frac{M_{\text{lo}}^{2m-2}}{M_{\text{hi}}^{2n+2m-1}}\,, \qquad \text{(NDA)}$$

$$g_1 \sim \frac{1}{M_{\text{hi}}}, \qquad h_{1+2m}\, m_\pi^{2m} \sim \frac{M_{\text{lo}}^{2m-1}}{M_{\text{hi}}^{2m}}\,,$$

$$\Delta \sim \frac{M_{\text{lo}}^{2}}{M_{\text{hi}}}\,, \qquad \omega_{2m}\, m_\pi^{2m} \sim \frac{M_{\text{lo}}^{2m+1}}{M_{\text{hi}}^{2m}}\,.$$

- A typical LEC: $\quad \mathsf{g} = \mathsf{g}^{(0)} + \mathsf{g}^{(1)} + \mathsf{g}^{(2)} + \dots\,,$
- The relation between phase shift and T matrix is

$$\delta^{(1)} = -k\,\overline{T}^{(1)} \qquad , \qquad \delta^{(2)} = -k\,\overline{T}^{(2)} - i\,k^2\,{\overline{T}^{(1)}}^2$$

P-waves: T matrix

- LECs at each order

$$\mathrm{LO} : - - -$$

$$\mathrm{NLO} : \Delta^{(0)},\ g_1^{(1)}$$

$$\mathrm{NNLO} : \tilde{\Delta}^{(1)} \equiv \Delta^{(1)} + \omega_2^{(1)}\, m_\pi^2,\ \tilde{g}_1^{(2)} \equiv g_1^{(2)} + h_3^{(2)}\, m_\pi^2,\ C_2^{(2)}$$

- NLO T matrix

$-i T^{(1)}$:

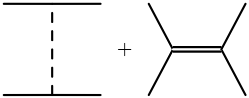

$$\Rightarrow \quad \overline{T}^{(1)}(k, m_\pi^2) = \overline{T}_\pi^{(1)}(k, m_\pi^2) + \frac{\eta\, m_N\, {g_1^{(1)}}^2\, k^2}{k^2 - m_N\, \Delta^{(0)}}\,.$$

P-waves: T matrix

- NNLO T matrix (see JBH (22) for more details)

$-i\,T^{(2)}$:

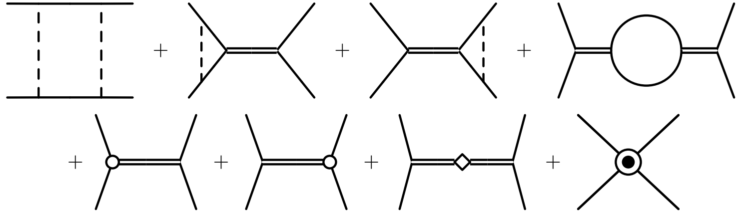

$$\overline{T}^{(2)}\left(k,m_\pi^2\right) = -i\,k\,\left[\overline{T}^{(1)}\left(k,m_\pi^2\right)\right]^2 + \mathcal{R}^{(2)}\left(k, g_1^{(1)}, \Delta^{(0)}, m_\pi^2\right)$$

$$+\frac{2\,\eta\,m_N\,{g_1^{(1)}}^2\,k^2}{k^2 - m_N\,\Delta^{(0)}}\left[I_{\pi d}^{[\mathtt{div}]} - \eta\,m_N\,{g_1^{(1)}}^2\,\frac{L_1}{2} + \frac{\tilde{g}_1^{(2)}}{g_1^{(1)}}\right]$$

$$+\,C_2^{(2)}\,k^2 - \frac{m_N^2\,{g_1^{(1)}}^2\,k^2}{\left(k^2 - m_N\,\Delta^{(0)}\right)^2}\left[{g_1^{(1)}}^2\left(L_3 + m_N\,\Delta^{(0)}\,L_1\right) - \eta\,\tilde{\Delta}^{(1)}\right].$$

P-waves: Renormalization and phase shift

- Two conditions for NNLO using data-point renormalization method

$$\mathrm{Re}\left[\overline{T}^{(2)}\left(k_{1,2}, m_\pi^2\right)\right] = \frac{\eta\, m_N\, \gamma^{(2)}\, m_\pi^2\, k_{1,2}^2}{k_{1,2}^2 - m_N\, \Delta^{(0)}} + \frac{\eta\, m_N^2\, {g_1^{(1)}}^2\, \theta^{(1)}\, m_\pi^2\, k_{1,2}^2}{\left(k_{1,2}^2 - m_N\, \Delta^{(0)}\right)^2}$$

- Total phase shift

$$-\frac{\delta^{(t)}}{k} = \overline{T}_\pi^{(1)}\left(k, m_\pi^2\right) + \frac{\eta\, m_N\, {\bar{g}_1^{(1)}}^2\, k^2}{k^2 - m_N\, \bar{\Delta}^{(0)}} + \mathcal{R}^{(2)}\left(k, g_1^{(1)}, \Delta^{(0)}, m_\pi^2\right) + \frac{(k^2 - k_1^2)\,(k^2 - k_2^2)}{\left(k^2 - m_N\, \Delta^{(0)}\right)^2}\, C_2^{(2)}\, k^2$$
$$- \frac{(k^2 - k_2^2)}{(k_1^2 - k_2^2)} \frac{\left(k_1^2 - m_N\, \Delta^{(0)}\right)^2}{\left(k^2 - m_N\, \Delta^{(0)}\right)^2} \frac{k^2}{k_1^2} \mathcal{R}_{k_1}^{(2)} + \frac{(k^2 - k_1^2)}{(k_1^2 - k_2^2)} \frac{\left(k_2^2 - m_N\, \Delta^{(0)}\right)^2}{\left(k^2 - m_N\, \Delta^{(0)}\right)^2} \frac{k^2}{k_2^2} \mathcal{R}_{k_2}^{(2)}$$

where $\bar{\Delta}^{(0)}$ and $\bar{g}_1^{(1)\,2}$ are

$$\bar{\Delta}^{(0)} \equiv \Delta^{(0)} + \theta^{(1)}\, m_\pi^2 = \Delta_{fit}^{(0)}$$
$$\bar{g}_1^{(1)\,2} \equiv g_1^{(1)\,2} + \gamma^{(2)}\, m_\pi^2 = g_{1\,fit}^{(1)\,2}$$

Results for ${}^1P_1$

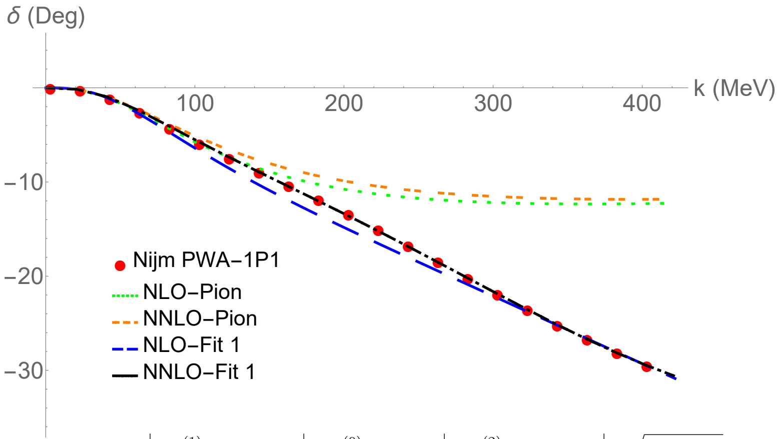

$^1\mathbf{P_1}$	$\{k_1, k_2, k_3\}$(MeV)	$g_{1_{fit}}^{(1)}$ (MeV^{-1})	$\Delta_{fit}^{(0)}$ (MeV)	$C_2^{(2)}$ (MeV^{-3})	$\sqrt{m_N\lvert\Delta^{(0)}\rvert}$ (MeV)	η
Fit 1	350, 400, 300	0.00112	-97.8	-3.8×10^{-9}	303.0	$+1$
Fit 2	310, 370, 280	0.00123	-149.2	-7.7×10^{-9}	374.3	$+1$

Results for $^3P_1$

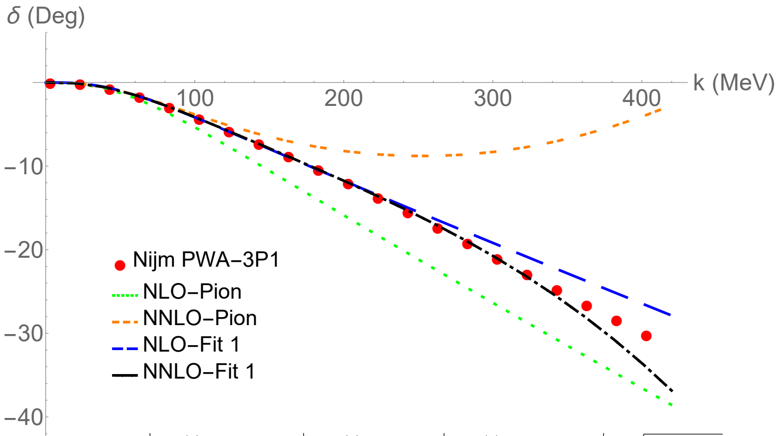

$^3\mathbf{P_1}$	$\{k_1, k_2, k_3\}$(MeV)	$g^{(1)}_{1_{fit}}$ (MeV^{-1})	$\Delta^{(0)}_{fit}$ (MeV)	$C^{(2)}_2$ (MeV^{-3})	$\sqrt{m_N\lvert\Delta^{(0)}\rvert}$ (MeV)	η
Fit 1	60, 200, 300	0.00071	-13.8	7.9×10^{-9}	114.0	-1
Fit 2	100, 250, 390	0.00065	-8.7	5.9×10^{-9}	90.4	-1

Results for $^3P_0$

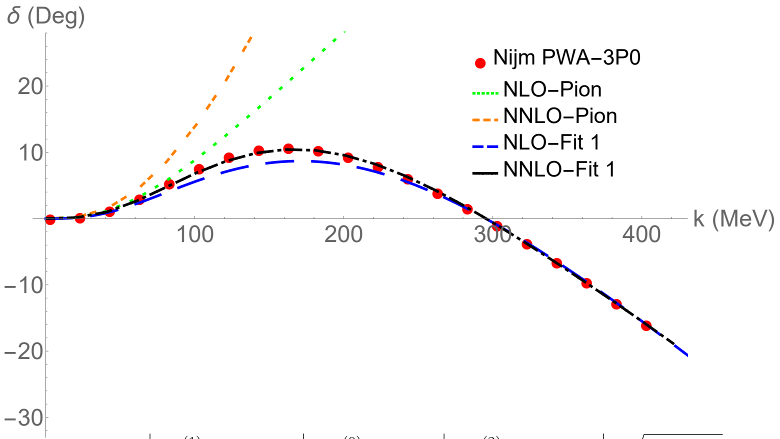

$^3\mathbf{P}_0$	$\{k_1, k_2, k_3\}$(MeV)	$g^{(1)}_{1_{fit}}$ (MeV^{-1})	$\Delta^{(0)}_{fit}$ (MeV)	$C_2^{(2)}$ (MeV^{-3})	$\sqrt{m_N\lvert\Delta^{(0)}\rvert}$ (MeV)	η
Fit 1	300, 400, 200	0.00250	-99.7	1.2×10^{-8}	305.9	$+1$
Fit 2	180, 320, 380	0.00286	-168.0	2.6×10^{-8}	397.2	$+1$

Other approaches for $^3P_0$

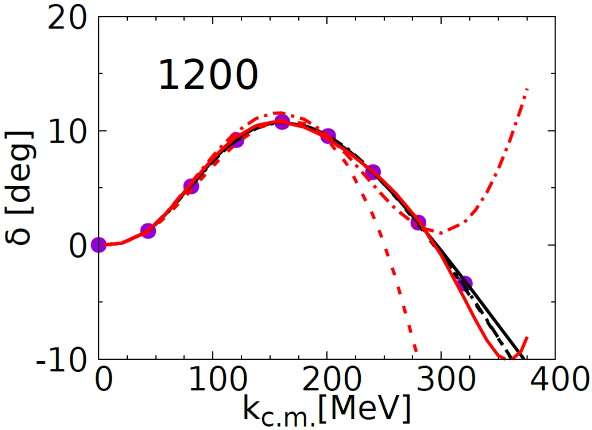

Figure 5: Phase shift for the $^3P_0$ channel. Perturbative (Red) and non-perturbative (black) EFTs. Red dashed, doted-dashed and solid lines are respectively NLO, NNLO, and N^{3}LO results for the perturbative case. Figures from Peng et al. (20).

Outline

Resonances in two body scattering

- Symmetries
  - Particle Number conservation,
  - Lorentz invariant (= Galilean + reparametrization)
  - Parity and time-reversal invariant
- Degrees of freedom: ψ (particles with mass m) and d (Dimeron).
- The most general S-wave Lagrangian (JBH et al. (21) [20])

$$\mathcal{L} = \psi^\dagger \left[i\,\partial_0 + \frac{\vec{\nabla}^2}{2m} \right] \psi + d^\dagger \left[i\,\partial_0 + \frac{\vec{\nabla}^2}{4m} - \Delta \right] d + \sqrt{\frac{4\pi}{m}}\,\frac{g_0}{4} \left(d^\dagger \psi\psi + \psi^\dagger\psi^\dagger d \right)$$
$$- \frac{4\pi}{m} C_0 \left(\psi\,\psi\right)^\dagger \left(\psi\,\psi\right) + \sqrt{\frac{4\pi}{m}}\,\frac{g_2}{4} \left[d^\dagger \left(\psi \overleftrightarrow{\nabla}^2 \psi \right) + \left(\psi \overleftrightarrow{\nabla}^2 \psi \right)^\dagger d \right]$$
$$+ \frac{4\pi}{m}\frac{C_2}{8} \left[(\psi\psi)^\dagger \left(\psi \overleftrightarrow{\nabla}^2 \psi \right) + \left(\psi \overleftrightarrow{\nabla}^2 \psi \right)^\dagger (\psi\psi) \right] + \dots\,,$$

Power counting

- In order to have resonant poles with Dimeron $m\,\Delta^{(0)} = \mathcal{O}\left(M_{\text{lo}}^2\right)$
- Broad resonances
  - Loops are non-perturbative because $k_I \sim k_R \sim M_{\text{lo}}$
  - Resummaiton needs $g_0^{(0)} = \mathcal{O}\left(\sqrt{M_{\text{lo}}/m}\right)$
  - Contact interactions can be natural $C_{2n} = \mathcal{O}\left(1/M_{\text{hi}}^{2n+1}\right)$
- Narrow resonances
  - Loops are perturbative because $k_I \ll k_R \sim M_{\text{lo}}$
  - Full perturbation needs $g_0^{(0)} = \mathcal{O}\left(\sqrt{M_{\text{lo}}^2/m\,M_{\text{hi}}}\right)$
- Broad resonances with amplitude zero
  - Loops are non-perturbative.
  - Contact interactions are promoted $C_{2n} = \mathcal{O}\left(1/M_{\text{lo}}^{n+1}\,M_{\text{hi}}^{n}\right)$

Broad Resonances

- LO and NLO diagrams

$-iT^{(0)}$:

$-iT^{(1)}$:

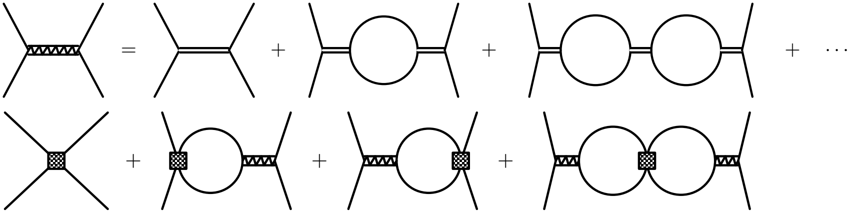

- LO and NLO T matrices with $r_0 < 0$ [20]

$$T^{(0)}(k) = \frac{4\pi}{m} g_0^{(0)2} \bar{D}^{(0)}(k) = -\frac{4\pi}{m}\left[-\frac{1}{a_0} + \frac{r_0}{2}k^2 - ik\right]^{-1} + \dots$$

$$T^{(0+1)}(k) = -\frac{4\pi}{m}\left[-\frac{1}{a_0} + \frac{r_0}{2}k^2 - P_0\left(\frac{r_0}{2}\right)^3 k^4 - ik\right]^{-1} + \dots$$

Broad Resonances

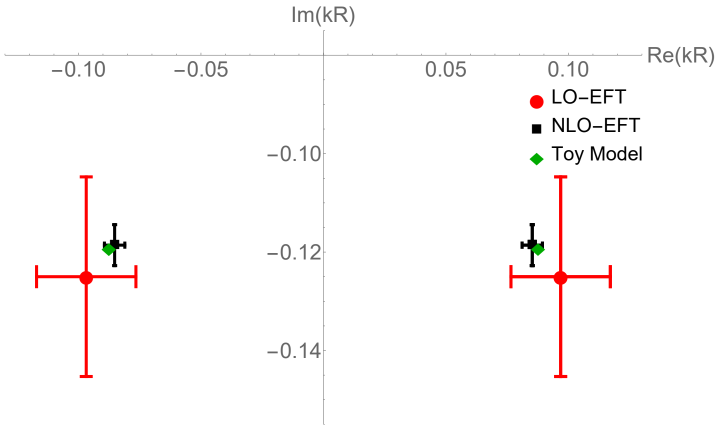

Figure 6: Comparing poles from EFT at LO and NLO with a toy model (as an underlying theory). In EFT, we have broad resonance when $r_0 < 0$ and $-2|r_0| < a_0 < 0$. For more details see JBH et al. (20) [21].

Narrow Resonances

- LO and NLO diagrams

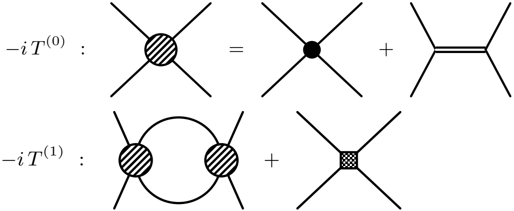

- LO and NLO T matrices [20]

$$T^{(0)}(k) = \frac{4\pi}{m}\left[C_0^{(0)} + g_0^{(0)2} D_0^{(0)}(k)\right] = \frac{4\pi}{m}\, a_0 \, \frac{k^2/k_0^2 - 1}{k^2/k_r^2 - 1}$$

$$T^{(0+1)}(k) = \frac{4\pi}{m}\left[\frac{1}{a_0}\,\frac{k^2/k_r^2 - 1}{k^2/k_0^2 - 1} + ik\right]^{-1} + \dots$$

Narrow Resonances

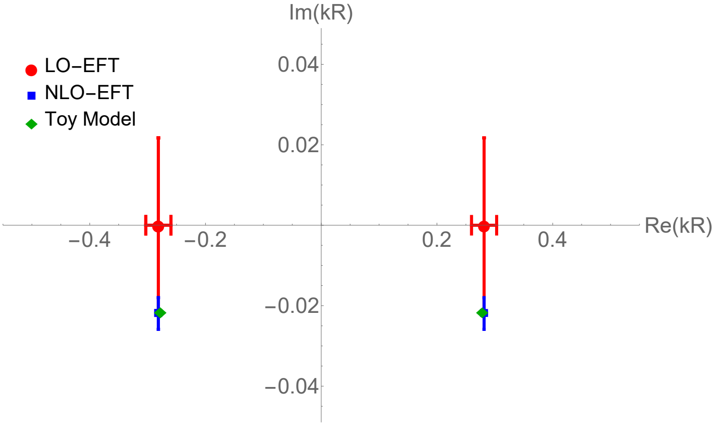

Figure 7: Comparing poles from EFT at LO and NLO with the same toy model now for narrow resonances ($k_I \ll k_R$). For more details see JBH et al. (21).

Braod Resonances with amplitude zero

- LO and NLO diagrams

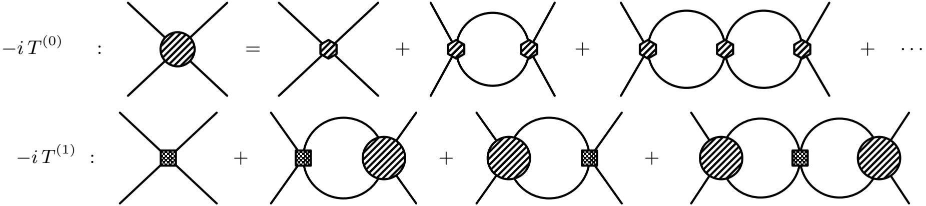

- LO and NLO T matrices [20]

$$T^{(0)}(k) = -\frac{4\pi}{m}\left[-\frac{1}{a_0} + \frac{r_0 k^2}{2}\frac{1}{1-k^2/k_0^2} - ik\right]^{-1} + \dots$$

$$T^{(0+1)}(k) = -\frac{4\pi}{m}\left[-\frac{1}{a_0} + \frac{r_0}{2}k^2 - \left(\frac{r_0}{2}\right)^3\frac{P_0 k^4}{1-k^2/k_0^2} - ik\right]^{-1} + \dots$$

Outline

Conclusion and Future Directions

- There is still a search for finding a correct PC that can explain hadronic physics below 1 GeV.
- One can use Dibaryon fields to address the convergence (and maybe the regulator-dependent) issues of the PC in the market.
- Dibaryon fields have been used in $^1S_0$ and uncoupled P-wave channels and (good) convergence to data has been observed.
- Dibaryon fields bring energy dependency into the potential. This makes it difficult for their applications in the many-body calculations. However, in few-body systems, Dibaryon fields make calculations a lot easier as long as one properly includes normalization factors.
- For pionless EFTs, a Dimer field is useful to study few-body systems (nucleons, atoms, ...) that show resonant behavior.

The End

Thank You

The toy model for resonances

- A potential with range R [20]

$$V(r) = \frac{\alpha}{mR}\,\delta(r-R) - \frac{\beta^2}{mR^2}\,\theta(R-r)$$

- S-wave phase shift

$$\cot\delta_0(k) = -\frac{(\sqrt{k^2R^2+\beta^2}\,\cot\sqrt{k^2R^2+\beta^2}+\alpha)\cot(kR)+kR}{\sqrt{k^2R^2+\beta^2}\,\cot\sqrt{k^2R^2+\beta^2}+\alpha-kR\cot(kR)}$$

- Zeros are given by

$$\sqrt{k_0^2R^2+\beta^2}\,\cot\sqrt{k_0^2R^2+\beta^2} = -\alpha + k_0R\cot(k_0R)$$

- Poles are given with

$$\sqrt{k_\pm^2R^2+\beta^2}\,\cot\sqrt{k_\pm^2R^2+\beta^2} = -\alpha + ik_\pm R$$

Narrow resonances from the toy model

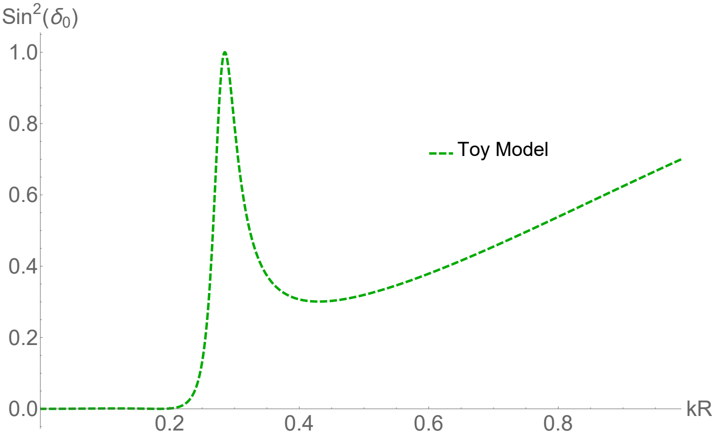

Figure 8: S-wave phase shift for the toy potential with $\alpha = 2\pi^2$ and $\beta = \pi^2 - 1$. Note that cross section is $\sigma \propto \sin^2 \delta_0$.

References I

[1] S. Weinberg. "Nonlinear realizations of chiral symmetry". In: *Phys. Rev.* 166 (1968), pp. 1568–1577.

[2] S. Weinberg. "Phenomenological Lagrangians". In: *Physica A* 96.1-2 (1979). Ed. by S. Deser, pp. 327–340.

[3] A. Manohar and H. Georgi. "Chiral Quarks and the Nonrelativistic Quark Model". In: *Nucl. Phys. B* 234 (1984), pp. 189–212.

[4] S. Weinberg. "Nuclear forces from chiral Lagrangians". In: *Phys. Lett. B* 251 (1990), pp. 288–292.

[5] S. Weinberg. "Effective chiral Lagrangians for nucleon - pion interactions and nuclear forces". In: *Nucl. Phys. B* 363 (1991), pp. 3–18.

References II

[6] D. B. Kaplan, M. J. Savage, and M. B. Wise. "Nucleon - nucleon scattering from effective field theory". In: *Nucl. Phys. B* 478 (1996), pp. 629–659. arXiv: nucl-th/9605002.

[7] D. B. Kaplan, M. J. Savage, and M. B. Wise. "A New expansion for nucleon-nucleon interactions". In: *Phys. Lett. B* 424 (1998), pp. 390–396. arXiv: nucl-th/9801034.

[8] D. B. Kaplan, M. J. Savage, and M. B. Wise. "Two nucleon systems from effective field theory". In: *Nucl. Phys. B* 534 (1998), pp. 329–355. arXiv: nucl-th/9802075.

[9] U. van Kolck. "Effective field theory of short range forces". In: *Nucl. Phys. A* 645 (1999), pp. 273–302. arXiv: nucl-th/9808007.

References III

[10] U. van Kolck. "Naturalness in nuclear effective field theories". In: *Eur. Phys. J. A* 56.3 (2020), p. 97. arXiv: 2003.09974 [nucl-th].

[11] A. Nogga, R. G. E. Timmermans, and U. van Kolck. "Renormalization of one-pion exchange and power counting". In: *Phys. Rev. C* 72 (2005), p. 054006. arXiv: nucl-th/0506005.

[12] S. Fleming, T. Mehen, and I. W. Stewart. "NNLO corrections to nucleon-nucleon scattering and perturbative pions". In: *Nucl. Phys. A* 677 (2000), pp. 313–366. arXiv: nucl-th/9911001.

[13] C. .-. Yang, A. Ekström, C. Forssén, G. Hagen, G. Rupak, and U. van Kolck. "The importance of few-nucleon forces in chiral effective field theory". In: (Sept. 2021). arXiv: 2109.13303 [nucl-th].

References IV

[14] D. B. Kaplan. "Convergence of nuclear effective field theory with perturbative pions". In: *Phys. Rev. C* 102.3 (2020), p. 034004. arXiv: 1905.07485 [nucl-th].

[15] D. B. Kaplan and J. V. Steele. "The Long and short of nuclear effective field theory expansions". In: *Phys. Rev. C* 60 (1999), p. 064002. arXiv: nucl-th/9905027.

[16] R. Peng, S. Lyu, and B. Long. "Perturbative chiral nucleon–nucleon potential for the $^3P_0$ partial wave". In: *Commun. Theor. Phys.* 72.9 (2020), p. 095301. arXiv: 2011.13186 [nucl-th].

[17] D. B. Kaplan. "More effective field theory for nonrelativistic scattering". In: *Nucl. Phys. B* 494 (1997), pp. 471–484. arXiv: nucl-th/9610052.

References V

[18] M. Sánchez Sánchez, C. .-. Yang, B. Long, and U. van Kolck. "Two-nucleon $^1S_0$ amplitude zero in chiral effective field theory". In: *Phys. Rev. C* 97.2 (2018), p. 024001. arXiv: 1704.08524 [nucl-th].

[19] J. B. Habashi. "Nucleon-nucleon scattering with perturbative pions: The uncoupled P-wave channels". In: *Phys. Rev. C* 105.2 (2022), p. 024002. arXiv: 2107.13666 [nucl-th].

[20] J. B. Habashi, S. Fleming, and U. van Kolck. "Nonrelativistic Effective Field Theory with a Resonance Field". In: *Eur. Phys. J. A* 57.5 (2021), p. 169. arXiv: 2012.14995 [hep-ph].

[21] J. B. Habashi, S. Sen, S. Fleming, and U. van Kolck. "Effective Field Theory for Two-Body Systems with Shallow S-Wave Resonances". In: *Annals Phys.* 422 (2020), p. 168283. arXiv: 2007.07360 [nucl-th].